

# An evaluation equation of load capacities for CFT square column-to-beam connections with combined diaphragm

Sung-Mo Choi<sup>†</sup> and Do-Sub Jung<sup>‡</sup>

*Department of Architectural Engineering, University of Seoul, Seoul, Korea*

Dae-Joong Kim<sup>‡</sup>

*Engineering & Construction Department of Samsung Corporation, Sungnam-Si, Kyungkido, Korea*

Jin-Ho Kim<sup>‡</sup>

*Research Institute of Industrial Science & Technology Steel Structure Research Laboratory,  
Kyungkido, 445-813, Korea*

*(Received February 14, 2006, Accepted May 14, 2007)*

**Abstract.** The objective of this study is to clarify the structural features of members consisting of connection, as a series of the previous study on the CFT column-to-beam tensile connection with combined cross diaphragm. This connection has the merits that the stress is distributed evenly on the beam flange and the diaphragm and the stress concentration is reduced, by improving the stress transfer route and restraining abrupt deformation of diaphragm. The finite element analysis was performed to find out the stress transfer through sleeve which is an important member of the connection with combined cross diaphragm. The length and thickness of sleeve were used as variables for the analysis. As the analysis results, the length and thickness of sleeve didn't influence on the capacity of the connection and played a role of a medium to transfer the stress from the diaphragm to the filled concrete. It is proposed that the appropriate length of sleeve be the same value as the diameter of sleeve and the appropriate ratio of sleeve diameter to sleeve thickness be 20. Two equations for evaluation of the load-carrying capacity of the connection were also proposed through the modification of the evaluation equation suggested in the previous study.

**Keywords:** concrete filled steel tube; combined cross diaphragm; sleeve; FEM; ANSYS.

---

## 1. Introduction

### 1.1 Research background

CFT structures feature structural excellence in strength and energy absorbing capacity due to the confinement effect on the filled concrete by steel tube and the restraint of local buckling of steel tube by

---

<sup>†</sup>Professor, Corresponding Author, E-mail: [smc@uos.ac.kr](mailto:smc@uos.ac.kr)

<sup>‡</sup>Research Associate

the filled concrete. CFT structures continue to show an increasing tendency to be used in low buildings and long-span structures as well as tall buildings.

The rigid connection is usually adopted in the CFT column-to-beam connection. If bending moment is applied to the beam in the CFT column-to-beam connection, the bottom of the connection is under compression and out-of-plane deformation of steel tube at the bottom of the connection can be restrained by the concrete inside the CFT column. But, the top of the connection is under tension and the concrete can't restrain out-of-plane deformation of steel tube. So, additional reinforcement is required at the top of the connection. Also, the capacity of CFT column-to-beam connection depends on its detail between column and beam flange.

Authors developed the CFT column-to-beam connection with combined cross diaphragm which penetrates the tensile flange of the column in the previous studies. These previous studies demonstrated the structural performance and seismic performance of the connection with combined cross diaphragm (Jung 2005, Cha 2003, Hong 2003, Choi 2004, 2005, Yoon 2002) and suggested the evaluation equation of load-carrying capacities of this connection (Choi 2004). In the previous studies, the evaluation equation was proposed through the experimental study only and the stress transfer through sleeve in the connection couldn't be proved clearly. Thus, the finite element analysis was carried out to confirm the mechanism of the stress transfer through sleeve in this study.

The length and thickness of sleeve were selected as variables for finite element analysis and the sensitivity of each variable was checked. Stress flow and plastic strain due to changing variables were also investigated. The analysis results were compared with the previous experiment results to verify the reliability of the analysis and the evaluation equation was completed by adding a condition for use to the existing evaluation equation.

### *1.2 Previous research*

The inner diaphragm and through-type diaphragm are mostly used in the CFT column-to-beam connection. If the connection with inner diaphragm is used in the long-span structures, the thickness of beam flange become thicker than thickness of column flange and excessive stress develops on the surface of column connected with beam. This can cause lamella tearing and early brittle failure.

To fabricate the connection with through-type diaphragm, the steel tube must be cut at the both levels of top and bottom beam flanges; then two diaphragms are inserted and welded to the beam flanges directly. This connection has a merit that stress transfer is clear but it requires cumbersome fabrication

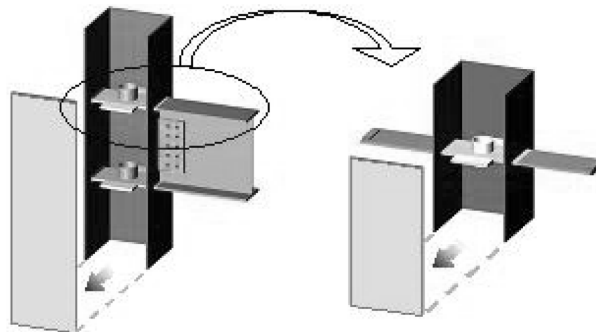


Fig. 1 CFT column-H shape beam connection and simple tension connection

process and welds work in field. If the beam flange is thick, the diaphragm becomes thick in proportion to the beam flange. So, welds work increases and quality control becomes difficult. Also, the brittle failure is anticipated for the stress concentration and the abrupt deformation of weld zone between diaphragm and beam flange.

The flange-through-type can be a good reference to the detail of CFT column-to-beam connection for the smooth stress transfer from the beam flange to the opposite side of the column, although it is usually applied to the connection of the RCS frame (Parra-Montesinos and Wight 2001) which consists of RC column and steel beam, not the CFT column-to-beam connection.

Azizinamini and Schneider (2004) demonstrated experimentally the performance of penetration detail of circular steel tube column in the beam-through-type CFT column-to-beam connection. In Japan, a connection that the filled concrete inside the CFT column was designed to resist the tension from the beam flange was developed. To fabricate this connection, two horizontal plates are inserted into both face of steel tube and a steel plate is added to the horizontal plates in T-shape to transfer the load to the filled concrete. This connection can transferred tension, only in a direction and have rather a smaller capacity than the other connection types.

Based on these previous researches, the connection with the combined cross diaphragm was developed to reduce out-of-plane deformation and abrupt form-change and improve the construction work. Fig. 2 illustrates the connection with the combined cross diaphragm. The load characteristic according to the ratio of long span to short span, that is, the asymmetric load transfer to the column due to the difference in spans of beams connected to the both sides of column was also considered in the detail of diaphragms as follows. In strong-axis where the larger bending force is applied, a diaphragm penetrates through the column flange and is connected directly to the beam flange. On the other hand, in weak-axis where the smaller bending force is applied, a diaphragm is inserted into the column, similarly to the connection with the inner diaphragm. Instead, the diaphragm in weak-axis has the same width as the beam flange. This can contribute to restraining the abrupt deformation and the stress concentration.

As the previous study (Cha 2002, 2003, Hong 2002, 2003, Choi 2004), the connection with combined cross diaphragm is more effective in initial stiffness and maximum capacity than the other types of

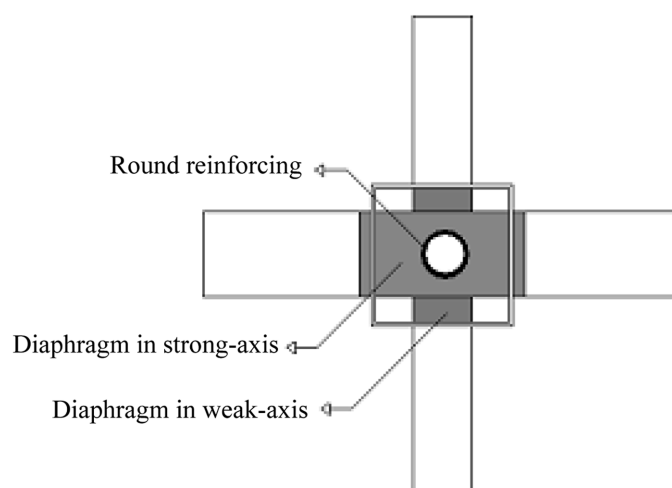


Fig. 2 Combined cross diaphragm

connection, under condition that they have the same opening size for filling the concrete into the steel tube. Also, it is also demonstrated that the stress is distributed evenly to the beam flange and diaphragm and the stress concentration on connection is reduced, by the improvement of stress transfer route and the detail restraining abrupt deformation of diaphragm.

## 2. Finite element analysis on connection

### 2.1 Analysis variables

The basic model of simple tension analysis in this study is the same as the test specimen in the previous study, as shown in Fig. 3. The analysis was carried out using ANSYS 8.0 (ANSYS Inc 2004) which is a universal finite element analysis program. The variables for analysis were the length and thickness of sleeve and the tendency according to each variable was checked. The length and thickness were expressed as the ratio of sleeve length to sleeve diameter and the ratio of sleeve thickness to diaphragm thickness, respectively. As shown in Table 1, the ratio of diameter of sleeve to width of beam flange was set as a variable and sleeve thickness had different values at each value of the variable. The capacity of connection and stress flow in connection according to the variation of the variable and sleeve thickness were investigated and the appropriate length and thickness of sleeve were suggested based on these analysis results.

### 2.2 Analysis modeling

Solid 65 element that has 8 nodes and 3 DOF (translational displacement for  $x$ ,  $y$  and  $z$  axis) at each node was used in the analysis. Fig. 4 illustrates the Solid 65 element. Besides, bi-linear Kinematic Hardening model that has VonMises' yield criterion and the characteristic of Bauschinger effect was used for the stress-strain characteristics of steel and concrete. It was assumed that the tangent modulus after yield of steel was 1/10 of Young's modulus and concrete was elasto-plastic material. The material properties of steel used in analysis was not the results of the material test but its nominal values. The values from Manual on design and construction of CFT structures were used for the Young's modulus and Poisson's ratio of concrete. These values are presented in Table 2.

In the boundary surface between steel tube and concrete, TARGET 170 element of 3-D Target Segment and CONTA174 of 3-D 8-Node Surface-to-Surface Contact element were used and the concrete was set to resist only compression through the surface-to-surface contact problem.

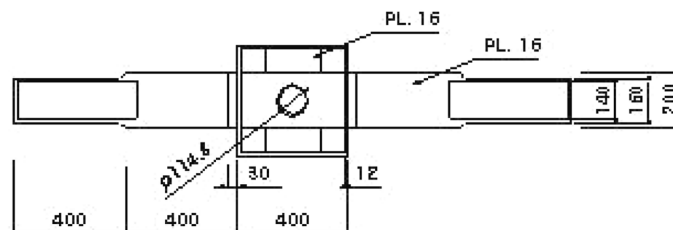


Fig. 3 Test specimen of existing study

Table 1 Analysis model list

$D_s/B_f$	$L_s/D_t$	$D_s/D_t$
		71
	0	36
0.6	0.2	19
	0.5	12
	1.14	9
	2	7
		71
0.4		25
		7
		71
0.5	1.14	25
		7
		71
0.7		25
		17

$D_s$ : Sleeve diameter,  $B_f$ : Width of beam flange,  $L_s$ : Sleeve length,  $D_t$ : Sleeve thickness

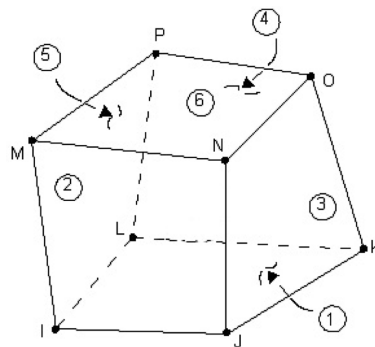


Fig. 4 Solid 65 element

Table 2 Material properties of simple tension analysis model element

Element	Steel Grade	$F_y$ (MPa)	Young's Modulus (GPa)	Tangent Modulus (GPa)	Poisson's Ratio
Steel tube	SM490	323.4			
Beam flange			2058	21	0.3
Diaphragm	SS400	235.2			
Round sleeve					
Concrete	-	49	299	0	0.167

In consideration of the symmetry of the connection and the load in the three perpendicular coordinate axes, the size of analysis model was set as 1/8 of test specimen as shown in Fig. 6 and the symmetry and boundary condition adjusted to this was given to the analysis model.

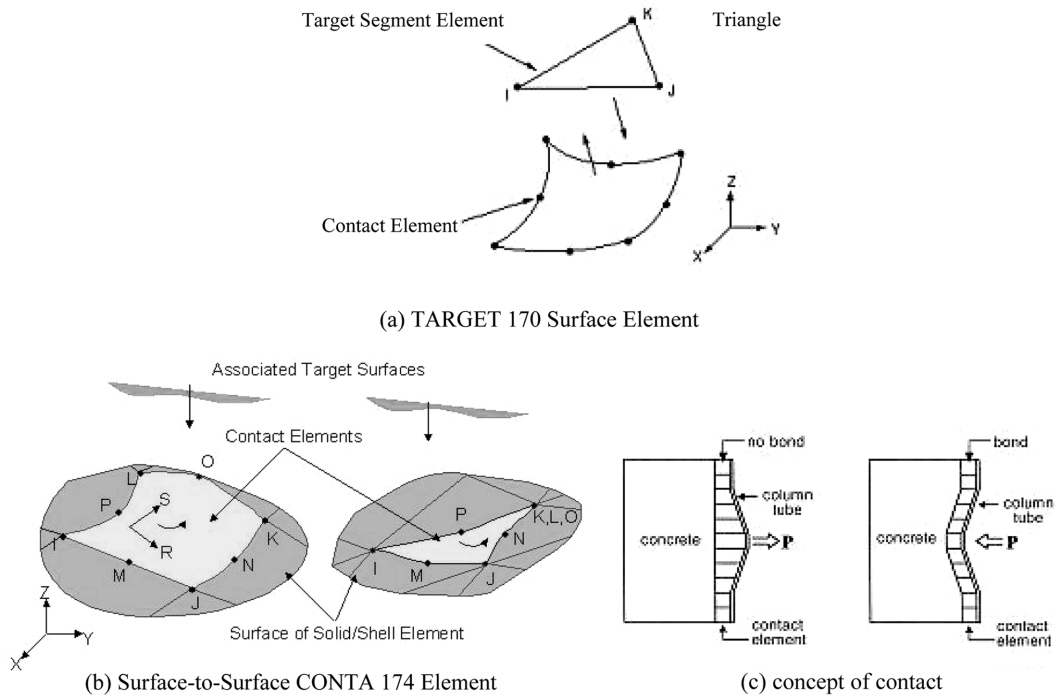


Fig. 5 Contact element

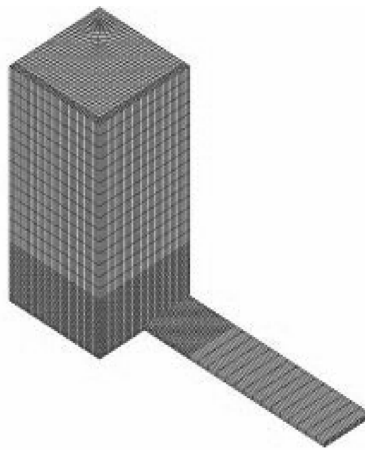


Fig. 6 Analysis model (1/8 model of specimen)

### 2.3 Verification of finite element analysis results

The reliability of finite element analysis results were verified through the comparison between the results of analysis and experiment.

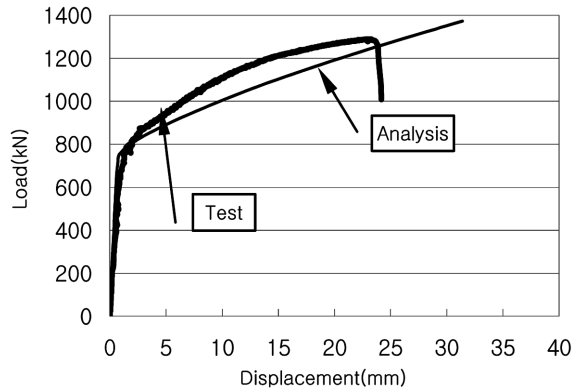


Fig. 7 Comparison between test and analysis results (Load-displacement curve)

### 2.3.1 Load-displacement curve

Fig. 7 shows the load-displacement curves obtained from the analysis and experiment. Two curves had nearly the same initial stiffness, but after yielding the curve from analysis was a little lower than one from experiment. It is thought that this is because the nominal values were used for the material properties in analysis, instead of material test results. But the tendencies of two curves were almost alike.

### 2.3.2 Strain distribution at each load step

Fig. 8 shows the strain distribution on the beam flange at each load step which was obtained from the analysis. The strain was distributed evenly on the width of beam flange like the experiment results.

### 2.4 Analysis results

Fig. 9(a) and (b) show the load-displacement curve obtained from the analysis according to the variation of sleeve length and sleeve thickness, respectively. The vertical axis represents the load applied to the beam flange and the horizontal axis represents the displacement of the surface of steel tube. (This is applied to all the following load-displacement curves) Besides, the variables in Fig. 9(a) are the ratios of sleeve length to sleeve diameter and the variables in Fig. 9(b) are the thickness-ratios of sleeve to beam flange.

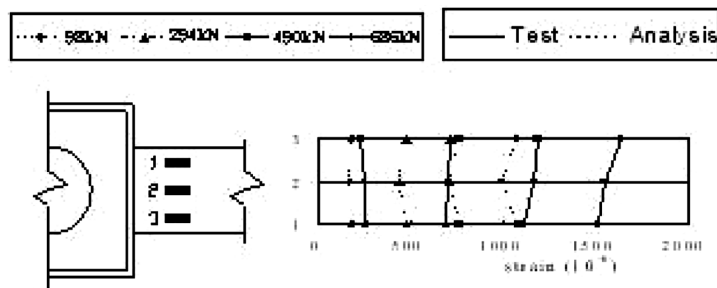


Fig. 8 Comparison between test and analysis results (Strain distribution on beam flange at each load step)

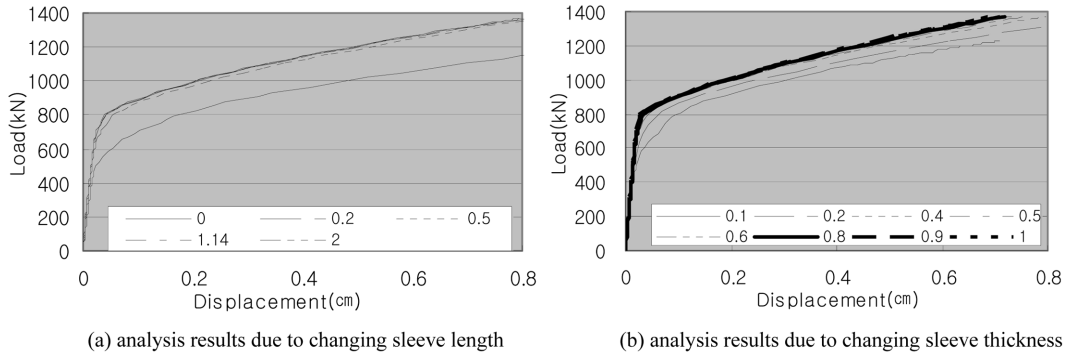


Fig. 9 Finite element analysis results

### 3. Analysis and consideration

#### 3.1 Capacity and stress flow according to the variation of sleeve length

Fig. 10 shows the relationship between load and displacement at the surface of steel tube due to changing length of sleeve. The variables in Fig. 10 are the ratios of sleeve length to sleeve diameter.  $P_{pf}$  represents the full-plastic load of beam flange (752.6 kN). It can be seen that the concrete filled in the steel tube resisted a portion of tension transferred from the beam flange due to the anchor effect of sleeve, for the curve of the connection without sleeve is much lower than the others. But, there wasn't much difference in capacities of connection with sleeve for the variation of the length of sleeve. Accordingly, it is considered that the thickness of sleeve doesn't influence on the capacity of the connection and the sleeve has only to obtain the length enough to generate the anchor effect.

The graph in Fig. 11 was obtained from dividing yield load of the connection in the load-displacement curve according to the variation of the sleeve length by full-plastic load of the beam flange. It can be seen that the yield load converges to a fixed value, if only the ratio of length to diameter of sleeve is 0.5 and above.

Fig. 12 shows the strain distributions on the diaphragm and the filled concrete according to the length of sleeve under the full-plastic load of beam flange (752.6 kN). Except the case without sleeve, strain

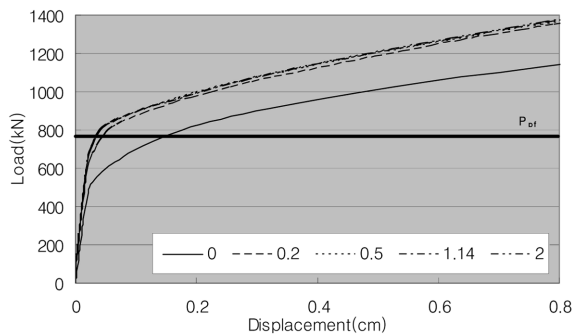


Fig. 10 Load-displacement curve due to changing sleeve length

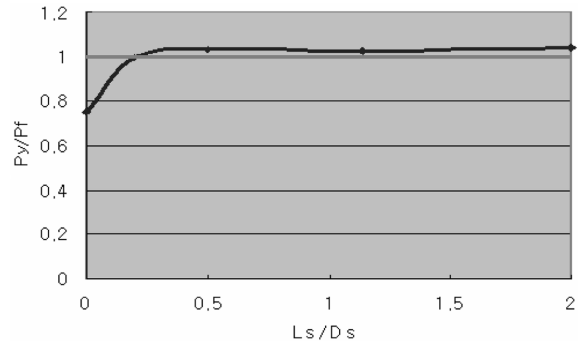


Fig. 11 Comparison of yield load due to changing sleeve length

*An evaluation equation of load capacities for CFT square column-to-beam connections with combined diaphragm 311*

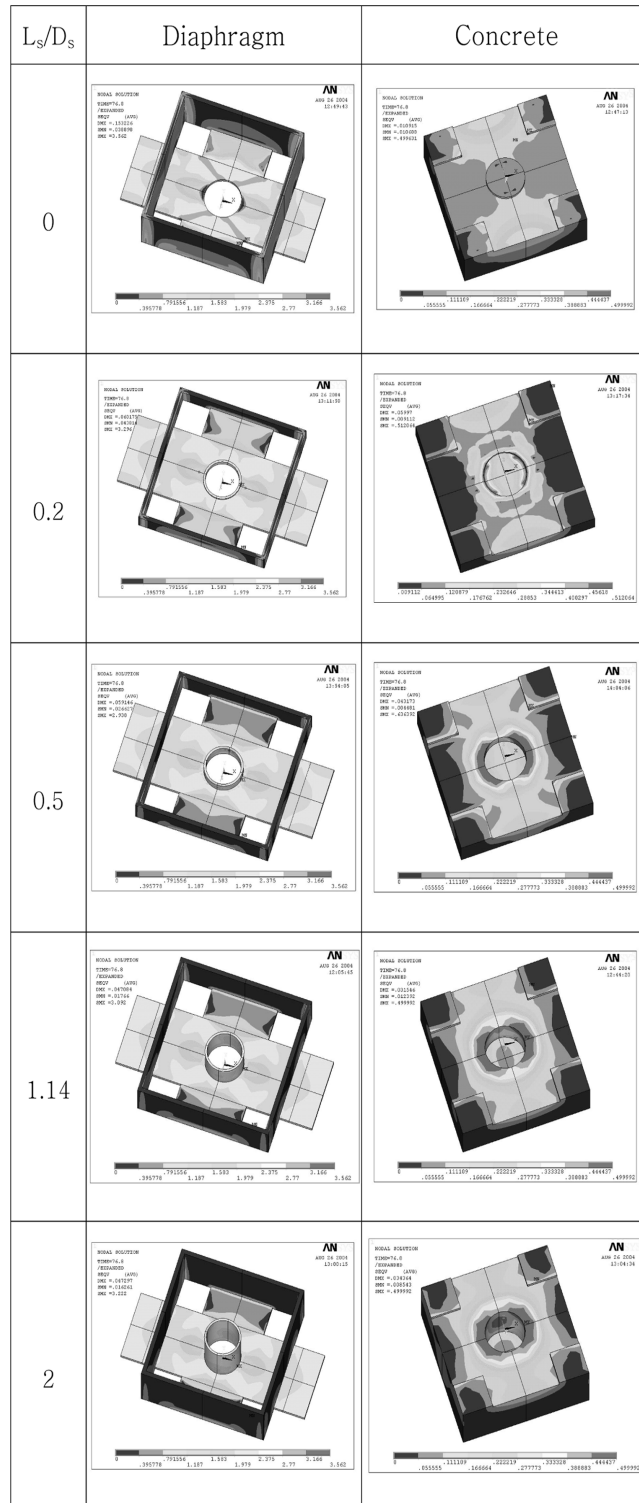


Fig. 12 Stress distribution on connection due to changing sleeve length

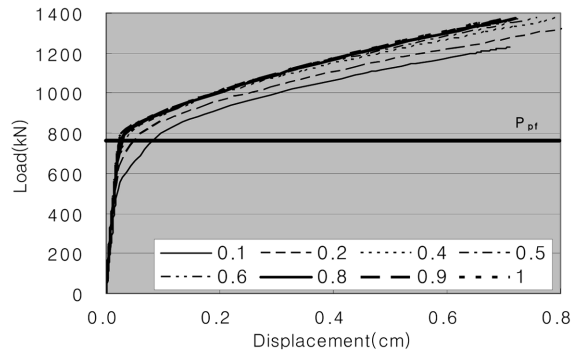


Fig. 13 Load-displacement curve due to changing sleeve thickness

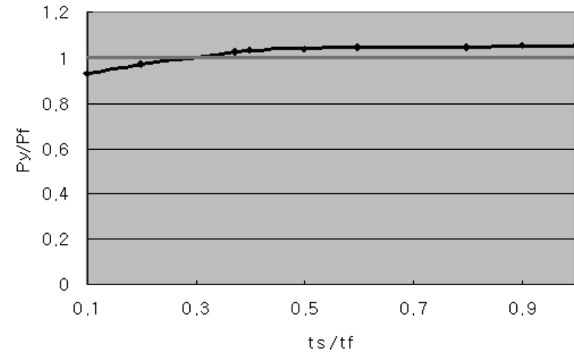


Fig. 14 Comparison of yield load due to changing sleeve thickness

distribution on the diaphragm was almost the same, irrespective of the length of sleeve. In the connection without sleeve, there wasn't much stress on the filled concrete. On the other hand, some stress developed on the center of concrete in the connection with sleeve. This is because the concrete resisted some tension from the beam flange through the anchor effect of sleeve. If the sleeve was short, anchor effect decreased and stress concentrated on the crossing of diaphragm. Thus, the diaphragm reached its maximum stress with the plastic state of crossing. But if the sleeve was long enough to generate the anchor effect, the stress was distributed on the concrete evenly. Authors propose that the appropriate length of sleeve be the same value as the diameter of sleeve.

### 3.2 Capacity and stress flow according to the variation of the sleeve thickness

Fig. 13 shows the relationship between load and displacement at the surface of steel tube due to changing the thickness of sleeve. The variables in Fig. 13 are the thickness-ratios of sleeve to diaphragm ( $D_s/B_f$ ). If the sleeve was thin, the anchor effect didn't generate sufficiently. On the other hand, if only the thickness ratio was 0.4 and above, the connection obtained sufficient capacity due to the smooth stress transfer through the sleeve and there wasn't much difference in capacity of connection, similarly to the case of sleeve length. Therefore, it is considered that the thickness of sleeve has only to be enough to exert anchor effect and doesn't affect the capacity of connection.

Fig. 14 is obtained from dividing yield load of the connection ( $P_y$ ) in the load-displacement curve due to changing the sleeve thickness by full-plastic load of the beam flange ( $P_f$ ). If only the thickness-ratio was 0.3 and above, the yield load converged to a fixed value.

Fig. 15 shows the stress distribution on diaphragm and concrete under full-plastic load of the beam flange (752.6 kN) due to changing the sleeve thickness. If thickness-ratio was 0.1 and below, the sleeve yielded early and concrete resisted only a small portion of tension. Thus, very thin sleeve can little exert the anchor effect. In addition, If thickness-ratio was 0.8 and above, little load was transferred to the concrete and the anchor effect decreased. It is thought that if the thickness-ratio is from 0.4 to 0.8, sleeve can exert the anchor effect well.

### 3.3 Suggestion of maximum ratio of sleeve diameter to sleeve thickness

The thickness of steel tube is limited by the ratio of the width or diameter to the thickness in steel

An evaluation equation of load capacities for CFT square column-to-beam connections with combined diaphragm 313

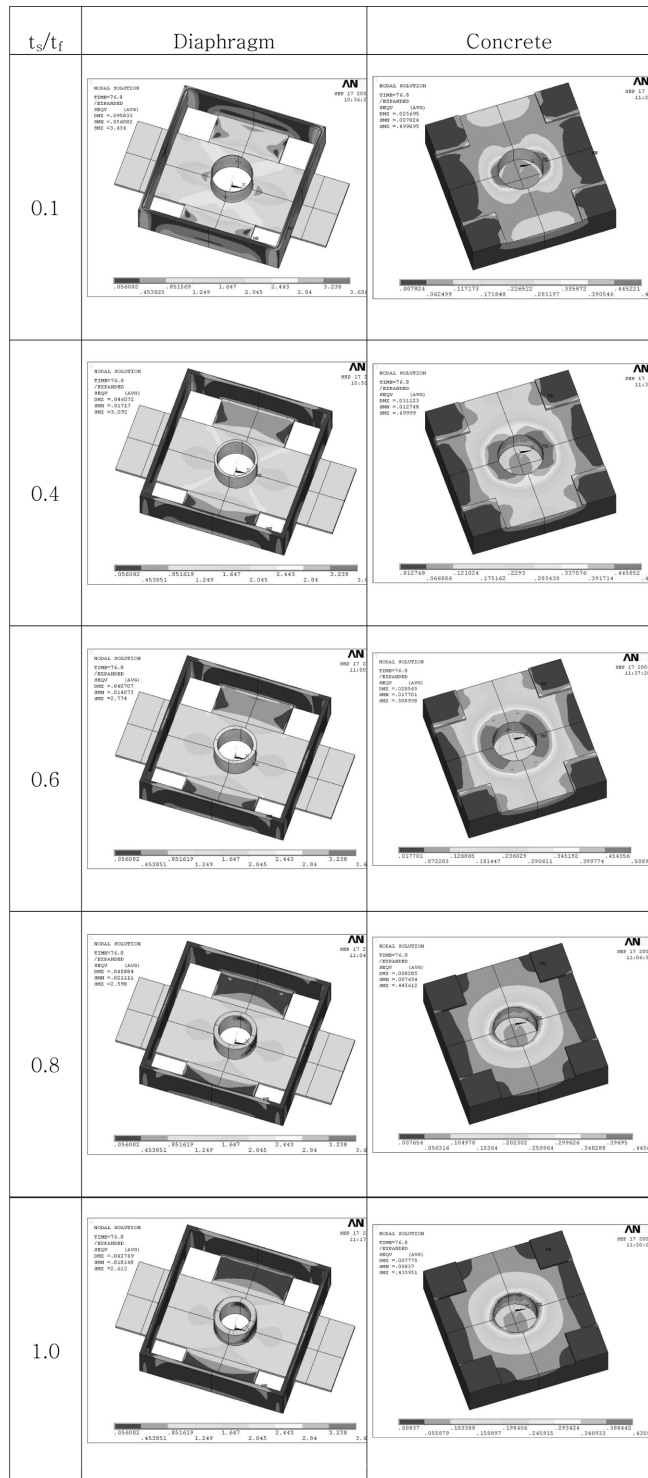


Fig. 15 Stress distribution on connection due to changing sleeve thickness

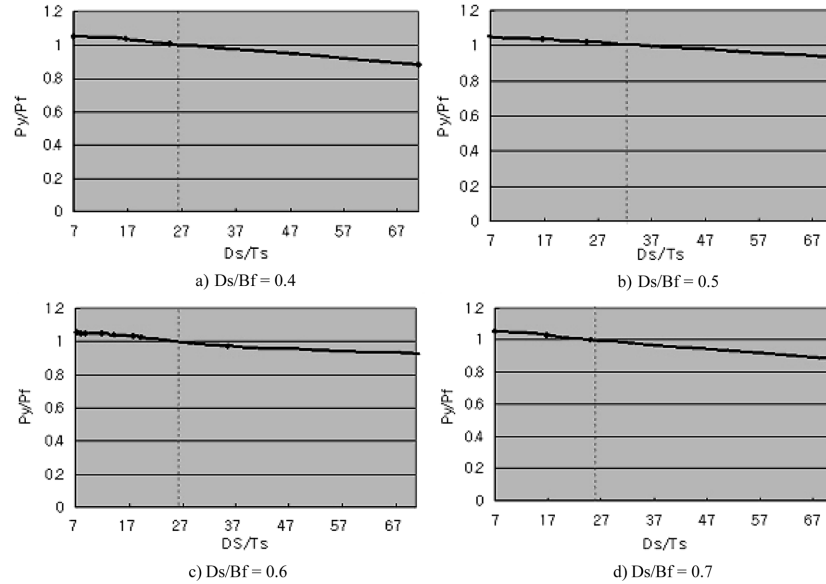


Fig. 16 Suggestion of sleeve diameter/thickness according to sleeve diameter/flange width

structures. In the design criterion of steel structure (Hong 2002), the ratio of the diameter to thickness is limited to 100 and below. To suggest the appropriate thickness of sleeve through the general expression on steel tube, the following work was carried out. First, the analysis results due to changing the thickness ratio of sleeve to beam flange were converted to those due to changing the ratio of sleeve thickness to sleeve diameter. Secondly, the analysis was carried out according to the sleeve thickness with varying sleeve diameter to generalize the maximum ratio of diameter to thickness.

#### 4. Evaluation equation of capacity of the connection with combined cross diaphragm

##### 4.1 Evaluation equation of load-carrying capacity

In the previous study, authors proposed two equations of evaluation of the load-carrying capacity of the connection with combined cross diaphragm, which were Eqs. (1) and (2) (Choi *et al.* 2004).

On the assumption that the yield capacity of the combined cross diaphragm is governed by two following failure modes, yield capacity is calculated at each failure mode. The yield capacity is determined as the smaller value between two calculated capacities.

Failure mode 1) Cone failure of concrete after yielding of the diaphragm

$$case1 P_y = [\sqrt{B_{sd}^2 + B_{wd}^2} - D] \cdot d F_y + \frac{1}{\sqrt{2}} \left[ \frac{3}{2} (B_c - 2t_c)^2 - \frac{D^2}{2} - (B_c - 2t_c) \right] \cdot v_c \quad (1)$$

Failure mode 2) Yielding of the flange of steel tube after yielding of the diaphragm

$$case2 P_y = [\sqrt{B_{sd}^2 + B_{wd}^2} - D] \cdot d F_y + t_c \left[ B_c + \frac{72t_c^2}{B_c - B_f} \right] \cdot \frac{c F_y}{6} \quad (2)$$

Here,  $P_y$ : Yield capacity of combined cross diaphragm (N/mm<sup>2</sup>)

$B_{sd}$ : Width of diaphragm in strong-axis

$B_{wd}$ : Width of diaphragm in weak-axis

$D$ : Diameter of sleeve

$dF_y$ : Yield strength of diaphragm

$cF_y$ : Yield strength of steel tube

$B_c$ : Width of steel tube

$t_c$ : Thickness of steel tube

$v_c$ : Shear strength of concrete

#### *4.2 Assumption used in evaluation equation of load-carrying capacity*

The previous evaluation equation is based on three following assumption. First, sleeve is considered only as a medium to transfer the tension to concrete. So it isn't included to the evaluation equation. Secondly, the cone failure of concrete by the tension transferred through the sleeve occurs in 45° direction, starting at the bottom where the stress concentrates, irrespective of the height of sleeve. And lastly, T.R. Higgins' model using the yield line method is adopted to evaluate the yield capacity of the flange of steel tube. The first and second assumption are proved to be appropriate based on the analysis in this study and the adequacy of the third assumption was already proved in the previous study (Choi 2004).

#### *4.3 Investigation of evaluation equation*

To test the validity of the evaluation equation proposed in the previous study, the yield capacities obtained through the finite element analysis and evaluation equation were compared with each other.

First, comparing the yield load due to each failure mode assumed in evaluation equation, the yield load of case 1 (yielding of the diaphragm + cone failure of the concrete) was much larger than one of case 2 (yielding of the diaphragm + yielding of the surface of steel tube using the yield line method). It is thought that the case 2 governs the capacity of the connection, for high-strength concrete is used usually to fill the steel tube in the CFT structure. Accordingly, it can be said that the primary failure mechanism of the connection with combined cross diaphragm is yielding of the flange of steel tube after yielding of the diaphragm.

Secondly, the yield load obtained from evaluation equation varied widely according to the sleeve diameter, while one from the finite element analysis was kept at an even value of about 784 kN. Therefore, it is considered that the yield mechanism assumed in the previous study must be modified.

#### *4.4 Modification of evaluation equation*

Fig. 17(a) and Fig. 18 show the plastic strain distribution on the connection and yield line of the diaphragm under the load of 752.6 kN, the full-plastic load of the beam flange, respectively. Fig. 17(b) shows the plastic strain distribution on the connection under the load of 1372 kN. The plastic deformation at the surface of the column didn't appear, but the connection exhibited its maximum capacity due to the deformation of the flange of steel tube according to yield line method after yielding of the diaphragm.

Table 3 Comparison of yield capacity 1

$D_s/B_f$	$L_s/D_s$	$D_s/D_t$	Yield Capacity(kN)		
			Analysis	Evaluation Equation	
				Case1	Case2
0.6	1	19	773.8	1259.6	926.5
		12	789.1		
		9	790.5		
		7	795.1		
0.4	1	25	763.3	1399	1055.6
		7	786.2		
0.5	1	25	767.2	1318.1	980.3
		7	796.2		
0.7	1	25	755.4	1152.7	829.8
		7	794.5		

$D_s$ : Sleeve diameter,  $B_f$ : Width of beam flange,  $L_s$ : Sleeve length,  $D_t$ : Sleeve thickness

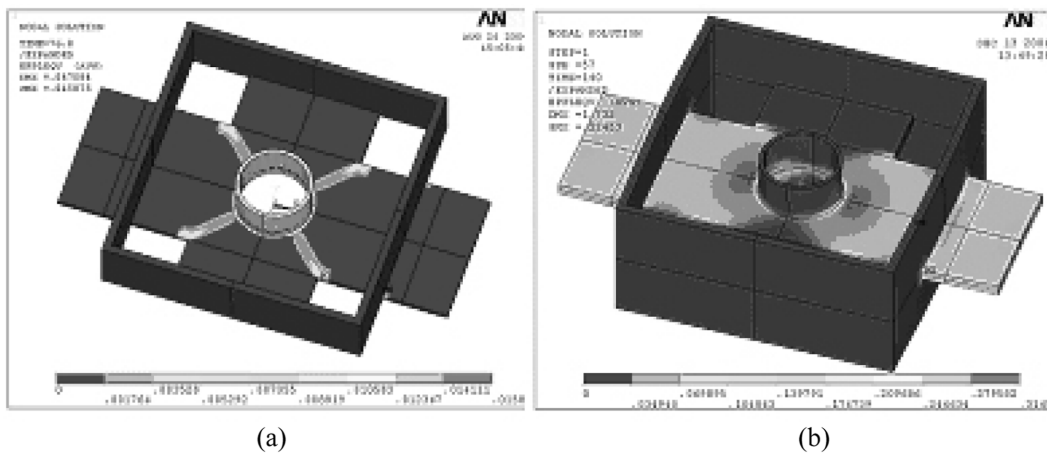


Fig. 17 Plastic strain distribution on diaphragm

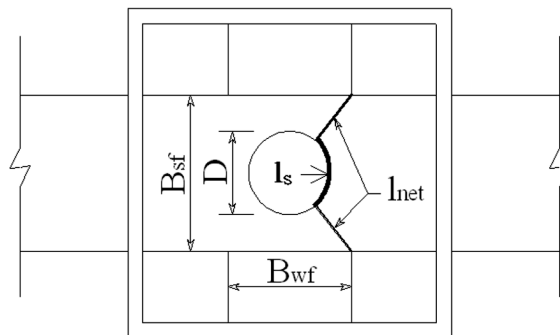


Fig. 18 Modified failure mode of diaphragm (1)

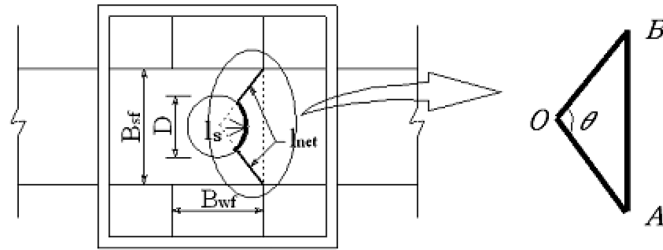


Fig. 19 Modified failure mode of diaphragm (2)

#### 4.5 Suggestion of modified evaluation equation of load-carrying capacity

As shown in Fig. 19, authors modified the failure mode of the diaphragm adding a part of opening (“ $l_s$ ”) to the existing yield line of the diaphragm (“ $l_{nel}$ ”). The length of  $l_s$  can be obtained from the Eq. (3), using the law of cosines.

$$l_s = r\theta$$

$$r = \frac{D}{2}$$

Applying the law of cosines to  $\Delta OAB$

$$\overline{AB}^2 = \overline{OA}^2 + \overline{OB}^2 - \overline{OA} \cdot \overline{OB} \cdot \cos \theta$$

$$\overline{OA} = \overline{OB} = \frac{\sqrt{B_{sf}^2 + B_{wf}^2}}{2}, \overline{AB} = B_{sf}$$

substituting

$$\cos \theta = \frac{B_{wf}^2 - B_{sf}^2}{B_{wf}^2 + B_{sf}^2}$$

$$\theta = \cos^{-1} \left( \frac{B_{wf}^2 - B_{sf}^2}{B_{wf}^2 + B_{sf}^2} \right)$$

$$\therefore l_s = \frac{D}{2} \times \cos^{-1} \left( \frac{B_{wf}^2 - B_{sf}^2}{B_{wf}^2 + B_{sf}^2} \right) \quad (3)$$

Therefore, the evaluation equation of yield capacity of the diaphragm can be expressed as Eq. (4).

$$P_{dy} = t_d \cdot (l_{nel} + l_s) \cdot dF_y$$

$$P_{dy} = t_d \cdot (\sqrt{B_{sf}^2 + B_{wf}^2} - D + l_s) \cdot dF_y \quad (4)$$

Here,  $P_{dy}$ : Yield capacity of combined cross diaphragm (N/mm<sup>2</sup>)

$l_s$ : Opening length included to the yield line (mm)

$l_{net}$ : Length of yield line of diaphragm (mm)

$B_{sf}$ : Width of the diaphragm in strong-axis (mm)

$B_{wf}$ : Width of the diaphragm in weak-axis (mm)

$D$ : Diameter of sleeve (mm)

${}_dF_y$ : Yield strength of diaphragm (N/mm<sup>2</sup>)

$t_d$ : Thickness of diaphragm (mm)

Authors propose Eq. (5) as the evaluation equation of ultimate capacity of the simple tension connection with combined cross diaphragm, adding the yield capacity of the flange of steel tube according to T.R. Higgins' yield line method.

$$P_u = t_d \cdot (\sqrt{B_{sf}^2 + B_{wf}^2} - D + l_s) \cdot {}_dF_y + t_c \cdot \left( B_c + \frac{72t_c^2}{B_c - B_f} \right) \cdot \frac{{}_cF_y}{6} \quad (5)$$

$$\text{here, } l_s = \frac{D}{2} \times \cos^{-1} \left( \frac{B_{wf}^2 - B_{sf}^2}{B_{wf}^2 + B_{sf}^2} \right)$$

The connection with combined cross diaphragm can be regarded to exhibit elastic behavior before yielding of the diaphragm. If the diaphragm in the connection is loaded to yield, this connection can't be reused. The connection exerts its ultimate capacity through the resistance of the steel tube after yielding of the diaphragm. So, it is thought that the yield capacity of the connection must be determined by the yield capacity of the diaphragm, in the design of the connection. As a result, authors propose the Eq. (6) as the evaluation equation of the yield capacity of the connection with combined cross diaphragm.

$$P_y = t_d \cdot (\sqrt{B_{sf}^2 + B_{wf}^2} - D + l_s) \cdot {}_dF_y \quad (6)$$

$$\text{here, } l_s = \frac{D}{2} \times \cos^{-1} \left( \frac{B_{wf}^2 - B_{sf}^2}{B_{wf}^2 + B_{sf}^2} \right)$$

#### 4.6 Investigation of modified evaluation equation

The yield capacities obtained through the finite element analysis were compared with those through modified evaluation equation. Table 4 gives the results of comparison of yield capacities. Their tendencies due to changing the diameter of sleeve are almost alike. So, it can be said that the modified evaluation equation is valid if adequate reduction factor is used. The results from the modified evaluation equation multiplied by reduction factor of 0.8 equals those from the finite element analysis, approximately. Finally, Eq. (7) and Eq. (8) are suggested as the evaluation equation of the yield capacity of the connection with combined cross diaphragm is proposed, using the reduction factor of 0.8.

Table 4 Comparison of yield capacity 2

$D_s/B_f$	$L_s/D_s$	$D_s/D_t$	Yield Capacity(kN)		
			Analysis	Evaluation Equation	Reduction Factor 0.8
0.6	1	19	773.8	972.1	777.6
		12	789.1		
		9	790.5		
		7	795.1		
0.4	1	25	763.3	999.7	799.9
		7	786.2		
0.5	1	25	767.2	983.6	786.9
		7	796.2		
0.7	1	25	755.4	951.3	761.1
		7	774.9		

$D_s$ : Sleeve diameter,  $B_f$ : Width of beam flange,  $L_s$ : Sleeve length,  $D_t$ : Sleeve thickness

Evaluation equation of ultimate capacity

$$P_u = 0.8 \cdot \left\{ t_d \cdot (\sqrt{B_{sf}^2 + B_{wf}^2} - D + l_s) \cdot {}_dF_y + t_c \cdot \left( B_c + \frac{72t_c^2}{B_c - B_f} \right) \cdot \frac{{}_cF_y}{6} \right\} \quad (7)$$

Evaluation equation of yield capacity

$$P_y = 0.8 \cdot \left\{ t_d \cdot (\sqrt{B_{sf}^2 + B_{wf}^2} - D + l_s) \cdot {}_dF_y \right\} \quad (8)$$

here,  $l_s = \frac{D}{2} \times \cos^{-1} \left( \frac{B_{wf}^2 - B_{sf}^2}{B_{wf}^2 + B_{sf}^2} \right)$

## 5. Conclusions

This study is on analysis of the structural performance of CFT column-to-beam connection with combined cross diaphragm. The conclusions by this study are as follows.

Combined cross diaphragm is the mixed type of through-type diaphragm and inner diaphragm. That is, in strong-axis, a diaphragm penetrates through the column flange and is connected directly to the beam flange. In weak-axis, diaphragm is inserted into the column and welded to the column, similarly to the inner diaphragm. Besides, the round opening is made in the center of the diaphragm for the good concrete-filling and cylindrical sleeve is welded to the diaphragm to compensate for the loss in sectional area of diaphragm.

If sleeve is used in the combined cross diaphragm, the yield capacity of diaphragm is expected to increase about 35%, due to the anchor effect of sleeve inserted to the combined cross diaphragm. The

length and thickness of sleeve don't influence on the capacity of the connection and have only to be enough to generate the anchor effect. Therefore, it is proposed that the appropriate length of sleeve be the same value as the diameter of sleeve and the appropriate ratio of sleeve diameter to sleeve thickness be 20.

This study suggested Eqs. (7) and (8) as the evaluation equations of the capacities of the connection with combined cross, modifying the failure mechanism of the connection and evaluation equation proposed in the previous study. It can be said that if the connection with combined cross diaphragm satisfies the proposed condition on the thickness and length of the sleeve, Eqs. (7) and (8) can be used for evaluation of the capacity of the connection.

## References

- ANSYS Inc. (2004), ANSYS Release 8.0-user's manual.
- Architectural Institute of Japan (1997), Recommendations for Design and Construction of Concrete Filled Steel Tubular Structures.
- Architectural Institute of Korea (1998), Design code and Explanation of Steel Tubular Structure.
- Architectural Institute of Korea (2004), Design and Construction Guide on Concrete Filled Tubular Structure.
- Azizinamini, Atorod and Schneider, Stephen P. (2004), "Moment connections to circular concrete- filled steel tube columns", *J. Struct. Eng.*, ASCE, **130**(2).
- Cha, E. J., Choi, S. M. and Kim, Y. S. (2003), "A moment-rotation curve for CFT square columns and steel beams according to reliability analysis", *ASSCCA*, 943-950.
- Cha, E. J., Kim, Y. S., Kim, J. H. and Choi, S. M. (2002), "Reliability analysis for CFT column-to-beam connections with new diaphragm", *Proceedings of International Symposium on Steel Structures: The Second*, 103-114.
- Choi, S. M., Hong, S. D., Kim, D. G., Kim, Y. S. and Kim, J. H. (2004), "Structural capacities of tension side for CFT square column-to-beam connections with combined cross diaphragm", *Pacific Structural Steel Conference*, 24-27, Mar., 2004.
- Choi, S. M., Kim, D. J., Kim, J. H. and Lee, S. H. (2005), "Experimental study on seismic performance improvement of concrete-filled tubular square column-to-beam connections with combined cross-diaphragm", *Int. J. Steel Struct.*, **5**(4), 367-375.
- Choi, S. M., Yoon, Y. S., Kim, D. K., Kim, Y. S. and Kim, J. H. (2004), "An experimental study on seismic performance of concrete filled tubular square column-to-beam connections with combined cross diaphragm", *Pacific Structural Steel Conference*.
- Davies, G and Packer, J. A. (1982), "Predicting the strength of branch plate-RHS connections for punching shear", *Canadian J. Civ. Eng.*, **9**(3), 458-467.
- Fung, T. C., Sho, C. K., Chan, T. K. and Erni (2002), "Stress concentration factors of doubler plate reinforced tubular T joints", *J. Struct. Eng.*, ASCE, **128**(11), 1399-1412.
- Hong, S. D., Choi, S. M. and Kim, Y. S. (2003), "A moment-rotation curve for CFT square columns and steel beams", *ASSCCA*, 951-960.
- Hong, S. D., Kim, Y. S., Kim, J. H. and Choi, S. M. (2002), "Simple tension testing for CFT column-to-beam connections at tension side with new diaphragms", *Proceedings of International Symposium on Steel Structures: The Second*, 405-416.
- Japanese Society of Steel Construction (1996), Design and Construction of Steel Beam-to-Column Connection - from the Earthquake Damage in the Southern Part of Hyogo-Ken.
- Jung, D. S., Choi, S. M., Kim, D. J. and Kim, J. H. (2005), "An experimental study on seismic performance improvement of concrete filled tubular square column-to-beam connections with combined cross diaphragm", *Proceedings of International Symposium on Steel Structures: The Third*, 524-535.
- Parra-Montesinos, G and Wight, J. K. (2001), "Modeling shear behavior of hybrid RCS beam-column connections", *J. Struct. Eng.*, ASCE, **127**(3).
- Yoon, Y. S., Kim, Y. S., Kim, J. H. and Choi, S. M. (2002), "Cyclic testing for CFT column-to-beam connections with new diaphragm", *Proceedings of International Symposium on Steel Structures: The Second*, 440-451.